A novel self-aligned process between a nano-aperture and a solid immersion lens for a near-field optical system

2006 J. Micromech. Microeng. 16 2632

(http://iopscience.iop.org/0960-1317/16/12/016)

INSTITUTE OF PHYSICS PUBLISHING JOURNAL OF MICROMECHANICS AND MICROENGINEERING

J. Micromech. Microeng. **16** (2006) 2632–2638 doi:10.1088/0960-1317/16/12/016

A novel self-aligned process between a nano-aperture and a solid immersion lens for a near-field optical system

Hung-Lung Hsu[1], **Yu-Ru Chang**[1], **Yi Chiu**[2], **Yu-Hsin Lin**[1,3] **and Wensyang Hsu**[1]

[1] Department of Mechanical Engineering, National Chiao Tung University, 1001 Ta Hsueh Road, Hsinchu 30010, Taiwan, Republic of China
[2] Department of Electrical and Control Engineering, National Chiao Tung University, 1001 Ta Hsueh Road, Hsinchu 30010, Taiwan, Republic of China
[3] Instrument Technology Research Center, National Applied Research Laboratories, 20 R&D Road VI, Hsinchu Science Park, Hsinchu 30010, Taiwan, Republic of China

E-mail: yhlin@itrc.org.tw

Received 25 June 2006, in final form 23 August 2006
Published 7 November 2006
Online at stacks.iop.org/JMM/16/2632

Abstract

For near-field optical systems, an aperture in nano-size and a solid immersion lens (SIL) are two popular methods to overcome the diffraction limit and reduce the optical spot size. In previous research, combining a nano-aperture and SIL has been proposed to provide high throughput and ultra-high resolution. However, alignment between the nano-aperture and SIL is very critical in the fabrication process, and no effective alignment technique has been investigated yet. In this research, a novel self-alignment technique is proposed for the combination of the nano-aperture and SIL, where the nano-aperture is fabricated with the focused ion beam (FIB) system and the SIL is formed by the thermal reflowing process. The self-alignment technique is based on the backside exposure and the surface tension self-modulation technique during the thermal reflowing process. The maximum deviation of the fabricated SIL is less than 3% in comparison with the designed values. A SIL of 15 μm diameter has been measured with 65.2% transmission efficiency. The polymer SIL combined with the circular aperture of 329 nm diameter has 1.68 times enhancement on throughput compared with the circular aperture of 329 nm alone. This result shows that the SIL can effectively enhance the throughput of the nano-aperture, and the feasibility of the proposed self-alignment method is also verified.

(Some figures in this article are in colour only in the electronic version)

1. Introduction

During the last decade, the technology of optical data storage has grown greatly. Due to the optical diffraction limit, the spot size of the conventional optical data storage system is directly proportional to the wavelength of incident light (λ) and inversely proportional to the numerical aperture (NA), which is equal to $n \sin \theta$, where n is the refractive index at the focal point and θ is the maximum incident angle of rays in the focused beam. In order to overcome the diffraction limit, various approaches have been developed and demonstrated toward near-field recording systems, where an aperture and a solid immersion lens (SIL) are two popular methods to reduce the spot size.

The aperture was introduced to optical storage by Betzig *et al* in 1992 [1]. In their approach, domains of 60 nm diameter in a magneto-topic material were written. In 1998, Pilevar *et al* [2] used a focused ion beam (FIB) to fabricate a 100 nm diameter aperture on a glass fiber coated with a 100–150 nm aluminum film. Since the spot size is directly

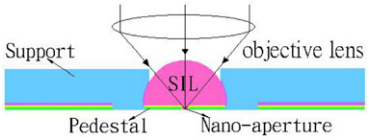

Figure 1. Concept design of the structure integrated with a nano-aperture and SIL.

determined by the aperture size, aperture systems can provide an ultra-high resolution by reducing the aperture size to nano-scale. However, the nano-aperture suffers low power throughput (10^{-4}–10^{-5}), which results in the recording speed unable to be promoted.

A SIL was introduced to decrease the spot size by Kino *et al* in 1990 [3]. In 2001, Lin *et al* [4] proposed to form a SIL by melting the photoresist. When the laser light focused by an objective lens is propagated into a SIL with a refractive index (n) > 1, the effective wavelength is reduced by a factor of n and the spot size focused onto the flat bottom surface of the SIL is reduced by the same factor. SIL systems can provide a smaller spot size than that obtained in conventional optical recording systems still maintaining high optical throughput.

In later research [5, 6], the nano-aperture combined with a SIL was shown to be able to enhance the power throughput over the aperture alone because the spot size illuminating the aperture is further focused by the SIL. However, the misalignment between the nano-aperture and SIL may occur in the assembling or bonding step, the result of which is that the light passing through the SIL will not focus on the nano-aperture. Hence, finding a way of aligning the nano-aperture and SIL without deviation becomes a key step to develop this integrated system. In this research, a reliable self-aligned process is proposed to overcome the misalignment between the nano-aperture made by FIB and SIL, based on the backside exposure and the surface tension self-modulation technique during thermal reflowing of the SIL on a glass wafer.

2. Concept design

A schematic diagram of the structure combined with the nano-aperture and SIL is shown in figure 1. The light is first focused through the objective lens, and then the spot size is shrunk by the SIL and nano-aperture. The wavelength of the light within the SIL becomes λ/n, so the final spot size focused on the bottom surface of the SIL by the objective lens can be shrunk by a factor of n in comparison with the structure without the SIL. In the proposed process, the integrated structure will be fabricated on a glass substrate with a sacrificial layer. The SIL on the pedestal is formed by thermal reflowing of the photoresist after proper front-side and backside exposures. The concentric patterns of the pedestal and nano-aperture are fabricated by FIB in the same step, so the concentricity is ensured by the resolution of the FIB system, which is about 7 nm in our case.

2.1. Self-aligned design of the nano-aperture and SIL

The key steps in the proposed self-alignment process are shown in figure 2. The nano-aperture and opening ring are concentric due to their FIB patterning in the same step. After the coated photoresist with proper thickness is exposed on the front side to define the diameter of the photoresist, as shown in figure 2(*a*), backside exposure is then performed with proper dosage, as shown in figure 2(*b*), to expose the photoresist beneath the pedestal in the opening ring region. After development, the columnar photoresist can be obtained, as shown in figure 2(*c*). Finally, the patterned photoresist is heated over its glass transition temperature, at which the liquid-like photoresist will tend to reduce its surface energy and become spherical in shape. By a suitable heat treatment time, the SIL can be formed, as shown in figure 2(*d*). Even though there will be an initial misalignment between the nano-aperture and the columnar photoresist in figure 2(*c*), the surface tension at the photoresist and interface can drag the liquid-like photoresist to the edge of the pedestal to eliminate the initial misalignment.

2.2. Design parameters of the SIL

In SIL dimensional designs, figure 3 shows the parameter definitions of the SIL. The volume of the photoresist shrinks during thermal reflowing. Therefore, a parameter of shrinkage ratio S is considered to minimize the deviation, where S is experimentally identified to be around 0.3. Equation (1) shows the required thickness of the columnar photoresist to form the

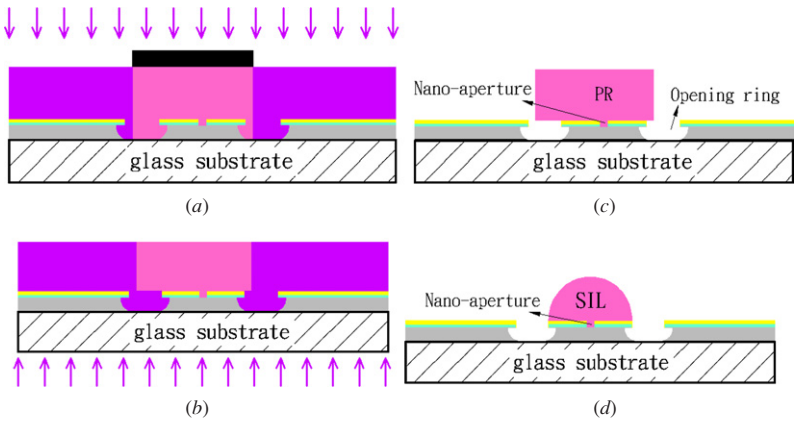

Figure 2. The self-alignment mechanism between the nano-aperture and SIL.

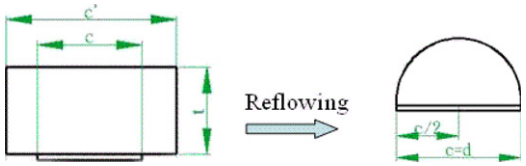

Figure 3. The schematic diagram of the design parameters of SIL.

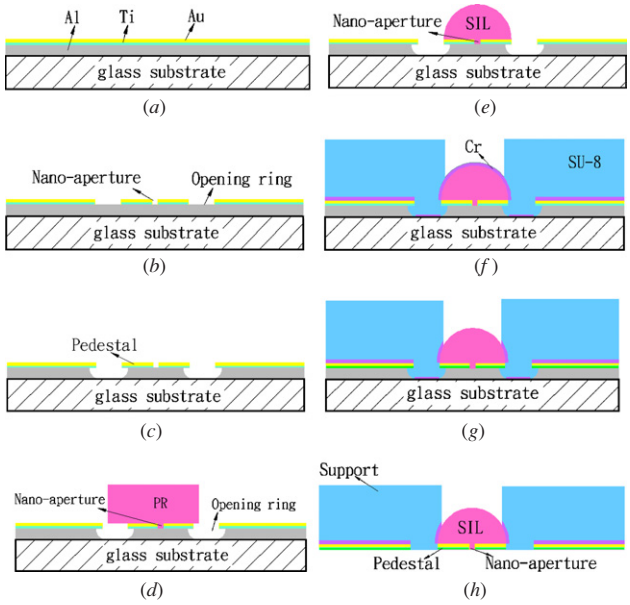

Figure 4. The fabrication flowchart of self-alignment between the nano-aperture and SIL.

SIL with diameter d:

$$t_{\mathrm{SIL}} = \frac{1}{3}\frac{d^3}{C'^2}\Big/(1-S). \tag{1}$$

3. Fabrication process

The fabrication flowchart is shown in figure 4. The SIL and nano-aperture are fabricated on a Pyrex glass wafer substrate. In figure 4(*a*), an aluminum (Al) film as a sacrificial layer is deposited by thermal evaporating on the glass wafer and a 20 nm titanium (Ti) film as an adhesion layer and a 200 nm gold (Au) film as a pedestal layer are then deposited by sputtering. After metal deposition, the nano-aperture and opening ring are patterned by FIB, which is a dual beam system (FEI NOVA 200 scanning electron microscope and focused ion beam), as shown in figure 4(*b*). The designed diameter of the pedestal is 15 μm and diameters of nano-apertures are 100 nm, 150 nm and 300 nm, respectively. It is noticeable that the ideal etching depth of the aperture and opening ring is controlled to just stop on the Al film. Nevertheless, over-etching is needed to ensure completely removing the Au/Ti films. Because the nano-aperture and opening ring are patterned in the same step, a concentric circle structure can be formed. Following FIB patterning, an Al etchant (80% H_3PO_4 + 5% HNO_3 + 5% CH_3COOH + 10% H_2O) is used to undercut the Al layer until the glass in the opening ring is exposed in figure 4(*c*). In order to fabricate the SIL, a positive photoresist AZ-4620 is chosen as the material of the SIL. The circular photoresist is defined in a mask aligner, and then backside exposure using the Au pedestal layer as a mask is performed. Since UV light can pass through the glass wafer and opening ring, the photoresist around the opening ring will be exposed. In this step, misalignment between the nano-aperture and columnar photoresist is inevitable, as shown in figure 4(*d*). By thermal reflowing at 190 °C, not only is the SIL formed, but the misalignment can be reduced by the surface tension force on the pedestal and photoresist interface to drag the liquid-like photoresist to the right position, as shown in figure 4(*e*).

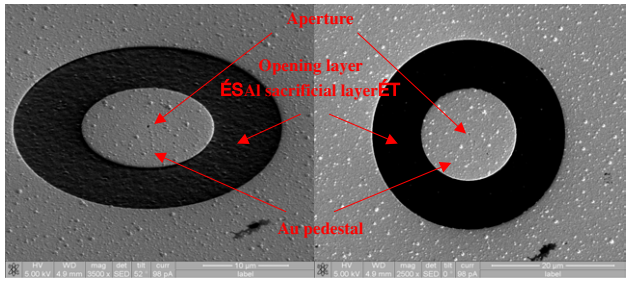

Figure 5. SEM image of the aperture and concentric opening ring by FIB patterning.

Following the SIL formation, the Cr cover layer is deposited by sputtering. The Cr film has two functions, one is to protect the solvent from permeating into the SIL during SU-8 coating and soft bake, and the other is to avoid the SU-8 developer to etch the SIL during development. Then a negative photoresist SU-8 as a support and connection component between the SIL and other part of the pick-up head is patterned, as shown in figure 4(*f*). In our case, when the thickness of the SU-8 support is 50 μm, the marginal ray angle will be about 7.5° where the maximum NA of SIL is 0.25. In order to make the light source pass through the SIL, the Cr film is etched in figure 4(*g*). Finally, the Al sacrificial layer is released by KOH, as shown in figure 4(*h*). The self-aligned SIL with a nano-aperture can be successfully made.

4. Experimental results and discussions

4.1. Formation of a circular nano-aperture and SIL

The diameter of the pedestal is designed to be 15 μm and diameters of the apertures are designed to be 100 nm, 150 nm and 300 nm, respectively. It is noticeable that the ideal etching depth of the aperture and opening ring is controlled to just stop on the Al film. Nevertheless, over-etching is needed to ensure completely removing the Ti/Au films. The scanning electron microscope (SEM) pictures of fabricated apertures with opening ring are shown in figure 5, where the Al layer is exposed after ion bombardment. Figures 6(*a*)–(*c*) show the close-up of fabrication results of apertures with diameters of 103 nm, 148 nm and 329 nm, respectively. Figure 7 shows the SEM of initial misalignment between the columnar photoresist and nano-aperture before thermal reflowing. After the thermal reflowing process, the SIL can be successfully formed and self-aligned with the nano-aperture, as shown in figure 8.

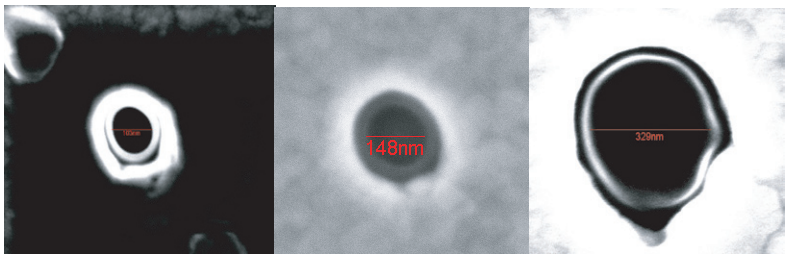

(*a*) (*b*) (*c*)

Figure 6. SEM images of the different dimensions of the circular aperture: (*a*) 103 nm; (*b*) 148 nm; (*c*) 329 nm.

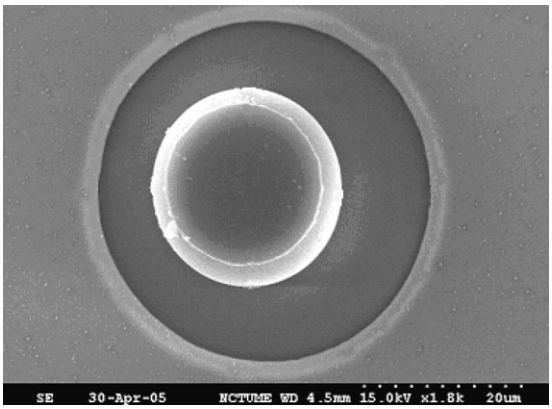

Figure 7. SEM images of the columnar photoresist before reflowing with misalignment.

The refractive index (n) and absorption coefficient (k) measured by spectroscopic ellipsometry are plotted in figures 9(*a*) and (*b*) as a function of wavelength for the photoresist film with different reflowing times. It is found that increasing the reflowing time will raise the refractive index and the absorption coefficient, which is particularly apparent at ultraviolet wavelength. It is believed that increasing the reflowing time will vaporize the residual solvent further in the photoresist film and increase the density of the photoresist. The refractive index almost does not change with the reflowing time over 6 h. The higher absorption coefficient means a lower transparency of the photoresist film relatively, which results in the lower light transmission efficiency through the same thickness of the film.

4.2. Optical measurement of the SIL with a circular nano-aperture

Due to the limitation of our available measurement equipment, only far-field measurements are conducted here, including the power throughput and spot size calibration. The schematic diagram of four measurement conditions is shown in figure 10 and the actual setup is shown in figure 11. The measurement equipment includes a 633 nm wavelength laser diode for providing the light source, a fiber lens for focusing the laser beam, an objective lens with 10 × magnification ratio (NA0.4) for collimating the output beam, a charge coupled device (CCD) for detecting the collimated output beam, a sensor for detecting light power, a power meter for measuring light power and an optical microscope for observing the position of the light spot focused by the fiber lens on the sample. During spot size measurement, the 633 nm laser beam is coupled and guided into the optical fiber and then focused by the front-end fiber lens whose focal length is about 200 μm with NA = 0.13. After light passes through the sample (SIL, aperture or SIL/aperture component), the output beam is collected and collimated by the objective lens whose focal length is about 1.6 cm. Finally, the collimated beam is detected by the CCD camera. The fiber lens, sample, objective lens and CCD camera are all set up on a three-axial position stage to ensure the alignment of the relative positions. The intensity profile of the collimated beam is converted from the captured CCD image by software.

In spot size calibration, the spot size focused by the fiber lens with or without a SIL can be calculated by the following equation:

$$D_{\text{spot}} = \frac{4f}{\pi d} \cdot \lambda, \tag{2}$$

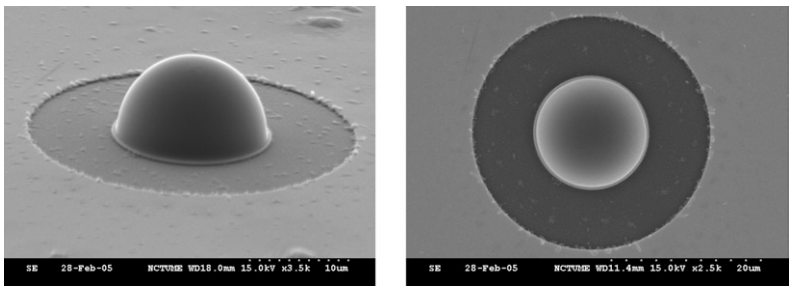

(*a*) (*b*)

Figure 8. SEM of (*a*) side view and (*b*) top view of the structure combined with a SIL and aperture without misalignment. SIL height = 7.57 μm and diameter = 14.57 μm.

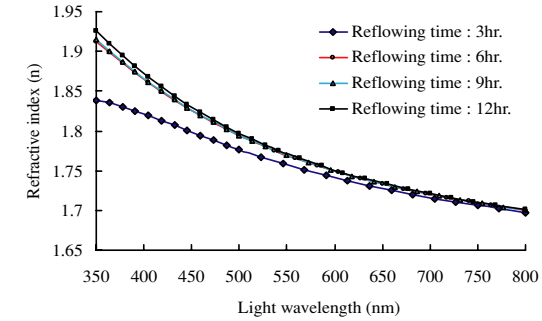

(*a*)

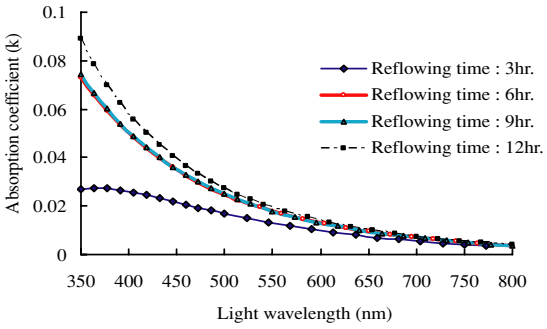

(*b*)

Figure 9. (*a*) The refractive index and (*b*) the absorption coefficient for the photoresist (AZ-4620) film as a function of light wavelength at 190 °C.

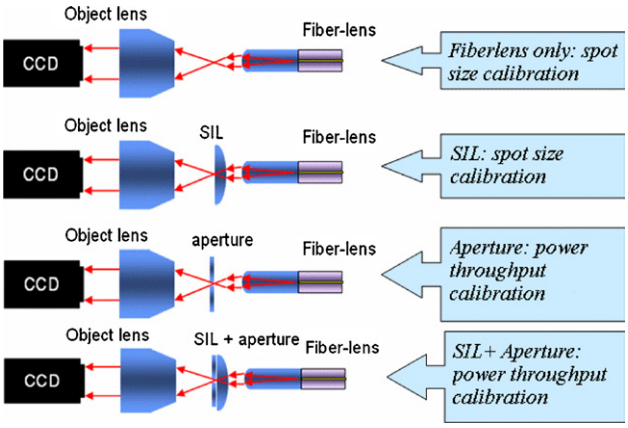

Figure 10. Schematic diagrams of the measurement system and four measuring conditions.

where D_{spot} is the spot size, f is the focal length of the objective lens, λ is the wavelength of the laser and d is the collimated beam size which is defined as full width at $1/e^2$ maximum intensity profile converted by the CCD camera. Since equation (2) would not work with the diffraction effect, spot size calibrations are performed only for the first two conditions in figure 10, where there is no nano-aperture involved.

In measuring power throughput, the power sensor is placed at the back of the objective lens to detect light power and then the detected signal will be transferred to the power meter. The power from ambient noise is found to be around 5 nW, which is relatively low.

The collimated beam profile focused by the fiber lens without and with the 15 μm diameter SIL is used to measure

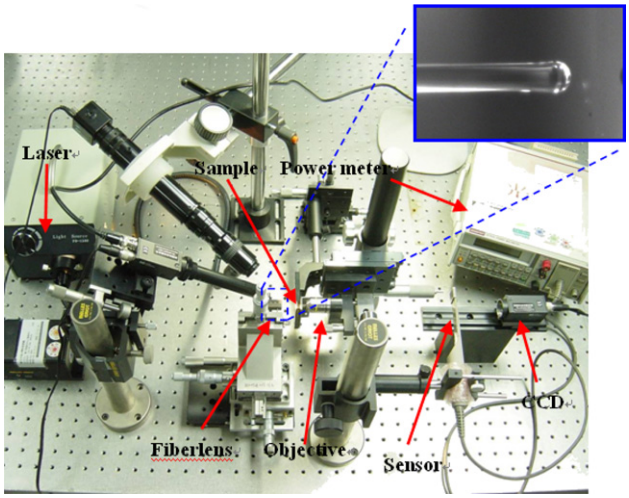

Figure 11. Optical measurement setup.

the shrink ratio of the spot size. The 15 μm diameter SIL can shrink the spot size 35.8%, which verifies that a SIL could focus the incident light and shrink the spot size at the bottom of the SIL. The weight of the liquid-like photoresist will resist its surface energy during the reflowing process, which may affect the profile of the SIL, whereas the weight effect can be diminished with a smaller SIL here.

Figures 12(*a*) and (*b*) show the intensity profile focused by the fiber lens with the circular aperture of 329 nm diameter and the 329 nm aperture with the 15 μm diameter SIL component, respectively. Equation (2) cannot be applied to obtain the spot size of the aperture because the spot size through the aperture is determined mainly by the dimension of the aperture and the light diffraction effect does not resemble the principle of focus. However, since the recording disk and near-field pick-up head have an air gap (or flying height), which will result in light diffraction effect during data storage, the spot size illuminating the disk will be larger than that passing through the aperture. It is apparent that the beam size in figure 12(*b*) is smaller than that in figure 12(*a*). This result indicates that the SIL can reduce the diffraction effect during light passing through the aperture and verifies the proposed self-aligned process.

Finally, the transmission throughput measurements are performed, where transmission is defined as the ratio of the total transmitted power through the aperture to the total incident power over the aperture area. In measurement, all samples have been measured for three cycles and the three measured results of each sample are averaged.

For the transmission efficiency of the SIL with 15 μm diameter, the input power is about 0.914 μW and then the measured output power is about 0.596 μW. Therefore, the throughput of the 15 μm SIL is 65.2%. By a similar measurement procedure, the throughput of the 15 μm SIL with the 329 nm aperture is found to enhance the light throughput 1.620 times in comparison with the 329 nm aperture alone. This result not only shows that the SIL can enhance the light power through the aperture, but also further verifies the feasibility of the proposed self-alignment method.

Table 1. Power throughput comparison for various apertures with and without a SIL.

Sample	Area (μm^2)	Transmission (output power/ input power)	Throughput (transmission/ area)(μm^{-2})
Circular aperture ($d = 329$ nm)	0.0769	1.838%	0.216
SIL + circular aperture ($d = 329$ nm)	0.0769	2.955%	0.350
Circular aperture ($d = 148$ nm)	0.0177	0.028%	0.0163
SIL + circular aperture ($d = 148$ nm)	0.0177	0.032%	0.0186
C-shaped aperture (205 nm × 303 nm)	0.0516	120.5%	0.2335
SIL + C-shaped aperture (205 nm × 303 nm)	0.0516	205.6%	0.3983

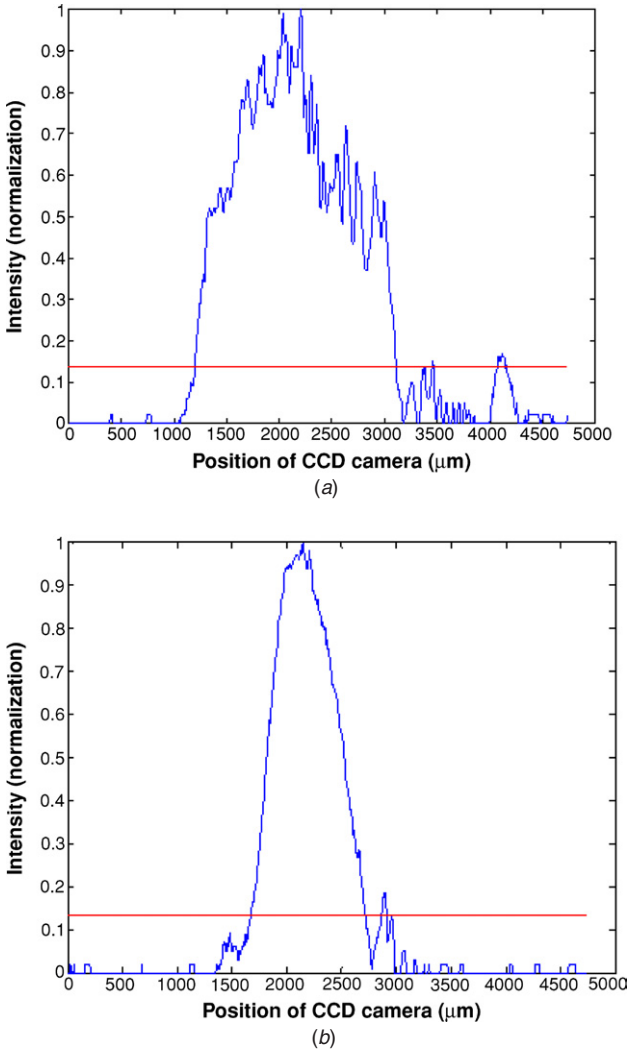

Figure 12. The measured output beam profiles which are (*a*) focused by the fiber lens with the aperture of 329 nm and (*b*) focused by the fiber lens and the aperture of 329 nm with the SIL of 15 μm.

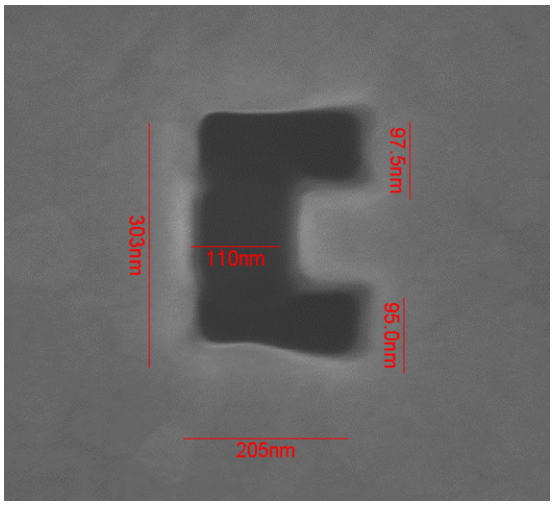

Figure 13. SEM image of the 205 nm (W) × 303 nm (L) C-shaped aperture.

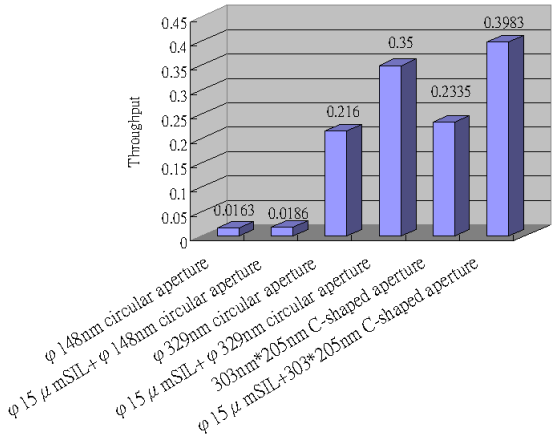

Figure 14. Throughput comparison of different types of apertures with or without the 15 μm SIL.

4.3. C-shaped nano-aperture

Besides combining the SIL with a circular nano-aperture, another type of aperture, a C-shaped aperture, as a ridge waveguide is fabricated to further enhance the power throughput. The C-shaped aperture has been shown to be able to overcome the large attenuation due to the cross-sectional area and exhibit waveguiding properties, overcoming the exponential decay with film thickness [7].

Here a C-shaped aperture with dimensions of 303 nm × 205 nm is also fabricated by FIB, as shown in figure 13, and then combined with a SIL. In measurement results of the C-shaped aperture, the throughput of the 303 nm × 205 nm C-shaped aperture alone is found to be 14.325 times larger than that of the 148 nm circular aperture with a similar near-field spot size. Furthermore, since a SIL can enhance the side incident light illuminating the C-shaped aperture, the throughput of the 303 nm × 205 nm C-shaped aperture combined with the 15 μm SIL is found to be further enhanced

by 24.438 times as compared with the 148 nm circular aperture alone. This result indicates that combining a SIL and C-shaped aperture can evidently enhance the performance of the near-field system. The throughput comparisons of the circular or C-shaped aperture with and without a SIL are shown in figure 14.

5. Conclusion

Here a self-alignment process based on the backside exposure and the surface modulation technique for the combination of a nano-aperture and SIL has been proposed and verified. The 15 μm SIL is formed by the thermal reflowing process and circular nano-apertures with 103 nm, 148 nm and 329 nm diameter are fabricated by FIB. It is shown that the 329 nm aperture combined with the 15 μm polymer SIL can enhance the throughput by 1.620 times in comparison with the 329 nm circular aperture alone at a wavelength of 633 nm. Furthermore, the throughput of the 303 nm $\times$ 205 nm C-shaped aperture combined with the 15 μm SIL is found to be 24.438 times larger than that of the 148 nm circular aperture alone, which verifies the feasibility of the proposed method to combine a SIL with different shapes of the nano-aperture.

Acknowledgments

This work was supported by the Ministry of Education of ROC for Promoting Academic Excellence of the University under grant no 89-E-FA06-1-4 and National Science Council grant NSC 90-2212-E009-033. Staffs at Instrument Technology Research Center for providing the focused ion beam system and Mr Jen-Yu Fang of the Optical Storage Laboratory at Institute of Opto-Electronic Engineering of National Chiao Tung University for assisting the measurements are also appreciated.

References

[1] Betzig E, Trautman J K, Wolfe R, Gyorgy E M and Finn P L 1992 Near-field magneto-optics and high density data storage *Appl. Phys. Lett.* **61** 142

[2] Pilevar S, Edinger K, Atia W, Smolynianov I and Davis C 1998 Focused ion-beam fabrication of fiber probes with well-defined apertures for use in near-field scanning optical microscopy *Appl. Phys. Lett.* **72** 3133–5

[3] Mansfield S M and Kino G S 1990 *Appl. Phys. Lett.* **57** 2615–6

[4] Lin Y S, Pan C T, Lin K L, Chen S C, Yang J J and Yang J P 2001 Polyimide as the pedestal of batch fabricated micro-ball lens and micro-mushroom array *14th IEEE Int. Conf. on Micro Electro Mechanical Systems*

[5] Fletcher D A, Simanovskii D, Palanker D, Crozier K B, Quate C F, Gorden S K and Goodson K E 2000 Microfabricated solid immersion lens with metal aperture *2000 IEEE/LEOS Int. Conf. on Optical MEMS*

[6] Milster T D, Akhavan F, Bailey M, Erwin J K, Felix D M, Hirota K, Koester S, Shimura K and Zhang Y 2001 Super-resolution by combination of a solid immersion lens and an aperture *Japan. J. Appl. Phys.* **40** 1778–82

[7] Shi X and Hesselink L 2002 Mechanisms for enhancing power throughput from planar nano-apertures for near-field optical data storage *Japan. J. Appl. Phys.* **41** 1632–5